

Improved threshold retracker for satellite altimeter waveform retracking over coastal sea *

GUO Jinyun^{1,2**}, HWANG Cheiway², CHANG Xiaotao³ and LIU Yuting²

(1. Department of Land Information and Surveying Engineering, Xuzhou Normal University, Xuzhou 221116, China; 2. Department of Civil Engineering, National Chiao Tung University, Hsinchu 30050, Taiwan, China; 3. Institute of Geodesy, China Academy of Surveying and Mapping, Beijing 100039, China)

Received October 21, 2005; revised January 23, 2006

Abstract Data quality is a key factor for the application of satellite altimetry to geodesy and oceanography. Accuracy of altimetry is limited in the coastal area because the altimeter waveforms are seriously contaminated by topography and environmental pollution. So waveform retracking is needed to compute the range correction of geophysical data records (GDRs) for better accuracy. In this paper, a new waveform retracker named the improved threshold retracker (ITR) is put forward. The retracker first builds sub-waveforms based on leading edges detected in a waveform, then determines the middle point of each leading edge to compute the retracking range correction, finally calculates the referenced sea surface heights according to the geoid undulation from a local geopotential model and tide heights from an ocean tide model, and compares it with all retracking ranges to determine the best one. As a test, altimeter waveforms of Geosat/GM are retracked around the Taiwan coastal area. The result shows that accuracy of ITR method is two times better than that of the β -5-parameter function-fitting method and threshold method, and three times better than that of GDRs. ITR can efficiently improve the altimetry accuracy of the coastal sea area.

Keywords: satellite altimetry, waveform retracking, improved threshold retracker, sub-waveform.

Determination of earth shape is one of the most important tasks of geodesy and geophysics. Earth gravity models express the geophysical shape of the earth, and geoids figure the geometric shape. The resolution of global gravity data obtained from the low-orbit satellite tracking is not high, only several hundred kilometers in half-wavelength. High resolution gravity data can be obtained by absolute and relative gravimetry in land areas, and by airborne and ship-borne gravimetry in mountain and coastal sea areas. For a wide open ocean, satellite altimetry is the best method to obtain gravity data of high accuracy and high resolution. Since the 1970s, satellite altimetry has provided abundant ocean data, which are widely applied to the study of the earth gravity model, mean sea surface, ocean tide model, seabed topography, and ocean wind and current^[1,2]. Now, more accurate altimetry data over seas, especially coastal seas are needed in the research. However, the returned pulse near lands is different from that of open oceans, because of the effect of coastal land topography, island and ocean tide which contaminate the al-

timetry waveform^[3]. Therefore, the waveform retracking is implemented in waveform data reprocessing to improve the range estimation of geophysical data records (GDRs). The main target of waveform retracking is to decrease the short-wavelength random noise, long-wavelength errors from sea significant wave height bias, range errors, instrumental errors, and errors from non-Gaussian sea surface. In coastal sea areas, altimetry accuracy becomes low because of the limited real-time data processing capability of the onboard tracker. Range errors from satellite orbits can be reduced by the dynamic, kinematic and combined methods^[2], and for the same reason those from the onboard tracker are also needed to be reduced. Since the returned waveform includes information from the sea surface, waveform retracking may improve the accuracy of altimetry ranging.

1 Waveform of satellite altimeter

The shape of returned pulse is the observation of satellite altimeter, which is a function with respect to two-way transmitting time and has a close correlation

* Supported by National Natural Science Foundation of China (Grant No. 40474004), Natural Science Foundation of Shandong Province (Grant No. Y2003E01), University Natural Science Foundation of Jiangsu Province (Grant No. 05KJB170129) and National Science Council, Taiwan (Grant No. NSC-93-2611-M-009-001)

** To whom correspondence should be addressed. E-mail: jinyunguo1@sohu.com; guojy@geodesy.cv.nctu.edu.tw

with the scattering characteristics of returned surface. Considering the vertical distribution of surface height and the effect of radar receiver, the mean returned pulse power $P(t)$, as a function of time delay, is a convolution of the probability density function of special point height on sphere and the point target response of radar system^[4], that is

$$P(t - t_0) = P_1(t - t_0) * q(t - t_0) * P_2(t - t_0), \quad (1)$$

where $*$ is a convolution operator; t is the time starting from pulse transmission; t_0 is the time of half power point; $P_1(t - t_0)$ is the mean pulse response on the flat surface; $P_2(t - t_0)$ is the point target response; $q(t - t_0)$ is the power density function of surface height within altimetry footprint. For the open ocean, the ocean surface approximately has the Gaussian distribution. Since the beamwidth of antenna is limited, Eq. (1) can be expressed as

$$P = \frac{1}{2} A [1 + \text{erf}(\eta)] Q(t), \quad (2)$$

where

$$\eta = \frac{t - t_0}{\sqrt{2}\sigma};$$

$$Q(t) = \begin{cases} 1, & t \leq t_0 \\ \exp[-(t - t_0)/\kappa], & t > t_0 \end{cases};$$

$$\text{erf}(\eta) = \frac{2}{\sqrt{\pi}} \int_0^\eta \exp(-x^2) dx;$$

σ is the rising time for pulse; A is the pulse amplitude maintained by automatic gain control (AGC); κ is the attenuation factor for the trailing edge of waveform. The target of waveform retracking is to determine the middle point of leading edge. Fig. 1 shows waveforms of Geosat/GM. Fig. 1(a) is an open ocean waveform, whose middle point of leading edge is consistent with the tracking gate. Figs. 1(b)—1(h) show some special waveforms when Geosat approaches land from open ocean or to ocean from land. Waveforms (b) and (c) present a spike or two spikes, (d) has several leading edges, (e) shows whose leading edge lags the tracking gate, (f) has the leading edge which is ahead of the tracking gate, and (g) and (h) are very irregular which make it very difficult to re-track.

Satellite altimeter calculates the range between the antenna and the sea surface with $\alpha - \beta$ tracker^[5]. AGC adjusts the waveform window to make the leading edge of returned pulse in the middle position of waveform samples at equivalent time interval. $\alpha - \beta$ tracker is

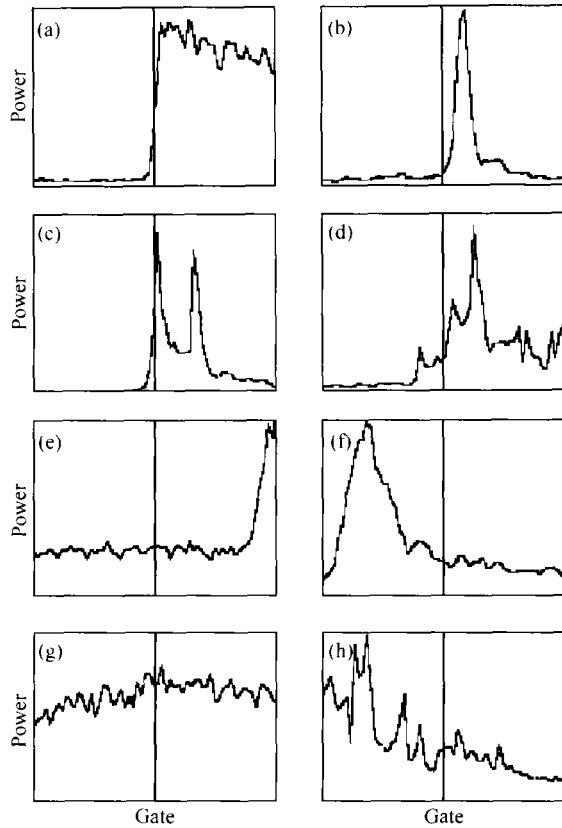


Fig. 1. Altimeter waveform shapes over coastal water. The upright line is the position of tracking gate, the transverse axis is the sampling gate, and the vertical axis is the sampling power.

$$r_{n+1}^p = r_n^p + \alpha \Delta r_{n-1} + \Delta t \dot{r}_n, \quad (3)$$

$$\dot{r}_n = \dot{r}_{n-1} + \beta \frac{\Delta r_{n-1}}{\Delta t}, \quad (4)$$

where r_{n+1} is the predicted range for the $n + 1$ -th tracking; r_n is the updated range for the n -th tracking; Δr_{n-1} is the range error for the $n - 1$ -th tracking of onboard tracker; \dot{r}_n and \dot{r}_{n-1} are the range rates for the n -th and $n - 1$ -th tracking, respectively; Δt is the time interval; α and β are tracking parameters. The observing ranges between satellite and sea surface in GDRs, which correspond to the tracking gate, are computed with $\alpha - \beta$ tracker. The tracking gate is fixed. For Seasat and Geosat, they are 30.5, and for ERS-1/2, TOPEX(Ku), GFO and Jason-1(Ku), they are 32.5, and for Poseidon and TOPEX(C), they are 29.5 and 35.5, respectively^[3]. Because of the waveform contamination, the middle point of practical leading edge is inconsistent with the tracking gate, as shown in Figs. 1(b)—1(h). In general, a waveform has only one leading edge. In practice, since the waveform is corrupted, a waveform may have many leading edges resulting from different reflecting surfaces, and the range dif-

ference from different leading edges may be up to meters.

The middle point of leading edge should be determined to calculate the range correction of waveform retracking, and so the range correction is applied to GDRs to compute more accurate range observation. Altimetry waveforms from ice-sheet can commonly be retracked with β -parameter function fitting method^[5], the offset center of gravity (OCO) arithmetic^[6], the threshold method^[7] and the surface-volume scattering retracker (SVSR)^[8], respectively. Supposing the returned pulse is Gaussian, β -parameter function fitting method uses 5- or 9-parameter function to fit the waveform with least squares method. The model has determinate physical meaning, but the surface of coastal water is not Gaussian. Therefore, the model is inapplicable to retrack the corrupted waveform. OCO is a simple waveform retracker based on the statistics of waveform. It is very easy for OCO retracker to retrack waveform, but its accuracy is low because the model is independent of the physical meaning of reflecting surfaces. Therefore, OCO is often used to calculate the initial values for β -parameter function fitting method. In threshold method, the threshold value should be firstly computed according to the power amplitude and the maximum sampling, then the retracked gate can be determined through the linear interpolation between the large slope part of waveform and the threshold value. The threshold method improves OCO to get a more accurate retracking gate. However, the threshold method has no physical meaning, and it is important and difficult to choose the best threshold value. For the open ocean, the percentage of threshold value is 50%, and for ice sheet, it is 20%^[7]. When the ice is covered by snow, radar pulse will permeate snow and then be reflected by ice, and so the returned pulse is summation of returned wave from snow and ice. SVSR is designed to retrack these kinds of waveform from ice sheet covered by snow. All the above retracking methods are designed to retrack waveforms from the ice sheet and open oceans. The surface of coastal water is different from that of ice sheet and open oceans^[3], so it is necessary to design a new waveform retracker to retrack the waveform from coastal water to calculate the more accurate altimetry range.

2 Basic retracking algorithms of linear β -5-parameter, OCO and threshold

Based on Eq. (1), a 5-parameter function is

used to fit single-ramp return waves. The retracking algorithm was used to process altimeter returned waveforms over continental ice sheets and to retrack all SEASAT waveforms to obtain corrected surface elevation estimates^[5]. The general linear β -5-parameter function is

$$y(t) = \beta_1 + \beta_2(1 + \beta_5 Q) P\left(\frac{t - \beta_3}{\beta_4}\right), \quad (5)$$

where,

$$Q = \begin{cases} 0 & t < \beta_3 + 0.5\beta_4 \\ t - \beta_3 - 0.5\beta_4 & t \geq \beta_3 + 0.5\beta_4 \end{cases}$$

$$P(x) = \int_{-\infty}^{\infty} \frac{1}{\sqrt{2\pi}} \exp(-0.5q^2) dq,$$

$$\beta_i (i = 1, 2, \dots, 5)$$

are unknown parameters, among which β_3 is the midpoint on the leading edge of waveform. Fitting waveform data, the unknown parameters can be estimated with the least squares method or maximum likelihood estimator.

Based on the definition of a rectangle about the effective center of gravity of waveform, the amplitude and width, the OCO retracking method uses full waveform samples to locate the half-power point as

$$LEG = \frac{\sum_i P_i^2}{\sum_i P_i} - \frac{1}{2} \frac{(\sum_i P_i^2)^2}{\sum_i P_i^4}, \quad (6)$$

where P_i is the sampled power.

The OCO retracking method is simple to implement, though it is purely statistical and is not based on any physical model of the reflecting surfaces. It is sensitive to the waveform shape affected by surface undulations and off-nadir pointing, because it uses the full samples in waveform bins. To improve the OCO estimation, the threshold method was used to process altimeter data from ERS satellite missions^[7]. The threshold method is based on the dimensions of OCO rectangle. The threshold value is then referenced to the amplitude or the maximum waveform sample estimate of the rectangle at 25%, 50% and 75% of the waveform amplitude. The retracking gate estimate is determined by linearly interpolating between adjacent samples of a threshold crossing at a steep part of the leading edge slope of waveform. The selection of an optimum threshold level is very important when applying the threshold method to waveform, but it is very difficult.

3 New waveform retracker: improved threshold retracker

A new retracker called improved threshold retracker (ITR) is put forward in this work. Based on the altimetry principle, the middle point of leading edge, which is the criterion for ranging timer, is corresponding to the half power of returned pulse. Therefore, a leading edge should be firstly searched, and a sub-waveform can be formed, then the middle point of sub-waveform can be determined and the retracked range correction can be calculated (see the following formulae (5)–(13)). There are probably many reflected surfaces, so a waveform may have many leading edges, but only one of which is corresponding to the nadir surface. Therefore, an exterior referenced height is needed to determine the best retracked range correction. For ocean waveform, the referenced height is the sum of the geoid anomaly calculated from earth geopotential model, dynamical sea surface topography (SST), and the tide height resulting from ocean tide model. For waveform returned from land and ice sheet, the referenced height results from the digital terrain model or the digital elevation model. Retracked sea surface height (SSH) will approach the referenced height datum, and retain some smooth and continuation with the former and latter SSHs.

When the fore of radar pulse arrives at sea surface, there is a light point on the reflected surface and the returned power starts to increase. When the rear of pulse touches the sea surface, there appears a largest solid light circle on the returned surface which indicates that the returned power is also largest. Then, there exists a light donut on the returned surface, and the returned power gradually makes attenuation. The leading edge of waveform locates between the light point and the largest solid light circle. The middle point of leading edge locates at the half point of the largest returned power. Therefore, the first job is to search all leading edges of the waveform.

Suppose that P_i is the returned power for the i -th gate. The mean difference between returned powers of spacing one is defined as

$$d_2^i = \frac{1}{2}(P_{i+2} - P_i). \quad (7)$$

The standard deviation for all differences of waveform powers of spacing one is

$$S = \sqrt{\frac{(N-2) \sum_{i=1}^{N-2} (d_2^i)^2 - \left(\sum_{i=1}^{N-2} d_2^i\right)^2}{(N-2)(N-3)}}, \quad (8)$$

where N is the maximum gate in the waveform.

If $d_2^i > 0.1S$, go on to resolve d_2^{i+1} . If $d_2^{i+1} > 0.1S$, continue to calculate d_2^{i+2} . When $d_2^{i+j-2} > 0.1S$, $d_2^{i+j-1} \leq 0.1S$ and $j \geq 3$, a leading edge is found with a doubt. Then the power difference between neighboring gates is defined as

$$d_1^k = P_{k+1} - P_k \quad (k = i, i+1, \dots, i+j-1). \quad (9)$$

The standard deviation of all single power difference for the waveform is

$$S_1 = \sqrt{\frac{(N-1) \sum_{i=1}^{N-1} (d_1^i)^2 - \left(\sum_{i=1}^{N-1} d_1^i\right)^2}{(N-1)(N-2)}}. \quad (10)$$

If $d_1^k > 0.1S_1$ for $k = i, i+1, i+j-1$, we think a real leading edge is found. If only one $d_1^k \leq 0.1S_1$ appears, we also think it a leading edge. Let $\tilde{P}_{k+1} = \frac{1}{2}(P_{k+2} - P_k)$ take the place of original P_{k+1} . If there are two single-differences dissatisfying the above condition, that is, $d_1^k \leq 0.1S_1$ and $d_1^{k+1} \leq 0.1S_1$, we think no leading edge is found.

Based on the above method, the waveform should be searched for all leading edges. For each leading edge, for example, $P_k (k = i, \dots, i+j-1)$, select n samples forward and backward from the i -th gate and $i+j-1$ -th gate, respectively, to form a new sub-waveform, that is, $P_k (k = i-n, i-n+1, \dots, i-1, i, \dots, i+j-1, i+j, \dots, i+j-1+n)$. As a matter of experience^[3], $n \leq 5$. For each sub-waveform, the retracked range correction can be calculated with the following equations as

$$A = \sqrt{\frac{\sum_i P_i^4}{\sum_i P_i^2}}, \quad (11)$$

$$P_N = \frac{1}{5} \sum_{i=1}^5 P_i, \quad (12)$$

$$T_L = \frac{1}{2}(A + P_N), \quad (13)$$

$$G_R = G_k - 1 + \frac{T_L - P_{k-1}}{P_k - P_{k-1}}, \quad (14)$$

$$\Delta R = R_0(G_0 - G_R), \quad (15)$$

where A is the power amplitude of sub-waveform; P_N is the thermal noise; T_L is called the threshold

level; G_k is the gate whose power is first greater than T_l for sub-waveform; G_R is the middle point of leading edge for sub-waveform; G_0 is the tracking gate; R_0 is the one-way range corresponding to the sampling interval; and ΔR is the retracked range correction.

Several leading edges may be found in one waveform and the corresponding retracked range corrections can be calculated through the above procedures. However, only one right retracked range correction exists in one waveform. Compared with a reference height, the best retracked range correction can be determined. For ocean, the referenced height is the sum of geoid anomaly, SST and tide height. The geoid anomaly can be calculated from the earth gravity model. The geopotential is expressed as spherical harmonic coefficients^[9]

$$V(r, \lambda, \phi) = \frac{GM}{r} \sum_{n=0}^{\infty} \sum_{m=0}^n \frac{R^n}{r^n} (\bar{C}_{nm} \cos m\lambda + \bar{S}_{nm} \sin m\lambda) \bar{P}_{nm}(\sin \phi), \quad (16)$$

where r , λ and ϕ are spherical coordinates (radial, longitude, and latitude); GM is the product of universal gravitation and the earth's mass; \bar{C}_{nm} and \bar{S}_{nm} are normalized geopotential coefficients; n and m are degree and order, respectively; \bar{P}_{nm} is the fully normalized Legendre polynomial; R is the earth radius. According to Bruns' equation, the geoid anomaly is expressed as

$$N = \frac{GM}{\gamma r} \sum_{n=0}^{\infty} \sum_{m=0}^n \frac{R^n}{r^n} (\bar{C}_{nm} \cos m\lambda + \bar{S}_{nm} \sin m\lambda) \bar{P}_{nm}(\sin \phi), \quad (17)$$

where γ is the normal gravity.

Since it is very difficult to distinguish the geoid anomaly from SST by the existing methods and data, the accuracy of the existing SST models is limited. The spatial resolution of SST is about tens of kilometers^[2]. For the retracked range correction, SST can be thought as a constant within tens of kilometers. SST is generally at the decimeter level, so the effect of SST can be neglected.

Ocean tide happens because of the gravitation effect of celestial bodies, such as sun and moon. The tide height from ocean tide model can be expressed as the spherical harmonic coefficients^[10]

$$h(\lambda, \phi, t) = \sum_s \sum_{n,m} P_{nm}(\sin \phi) [C_{nm}^+ \sin(\theta_s + \epsilon_{snm}^+ + \chi_s + m\lambda) + C_{nm}^- \sin(\theta_s + \epsilon_{snm}^- + \chi_s - m\lambda)], \quad (18)$$

where t is time in MJD; s is the tide wave; n , m are

degree and order, respectively; C_{snm}^{\pm} is amplitude; θ_s is argument of ocean tide; ϵ_{snm}^{\pm} is the phase of ocean tide; χ_s is the ocean tide constant relative to amplitude.

4 Waveform retracking of GEOSAT/GM over coastal seas around Taiwan Island

Coastal waters around Taiwan Island are chosen as the test area in this work, as shown in Fig. 2. East of Taiwan, the collision of the Eurasia Plate and the Philippine Sea Plate create islands and complex shorelines. Here, the depth of the Pacific Ocean plunges to 4 km just about 10 km to 20 km off the east coast of Taiwan. West of Taiwan lies the Taiwan Strait, where the deepest part is only 50 m and the water is scattered with islands and barrier islands. The East China Sea, not deeper than 200 m and also scattered with islands, lies north of Taiwan. The South China Sea is to the south of Taiwan and there exists a small island called Liuchou, which might interfere with altimeter waveforms. Many other islands locate around Taiwan, such as Penghu, Lanyu, Ludao, and Guishan. Therefore, the coastal water around Taiwan becomes an ideal test area for altimetry waveform retracking.

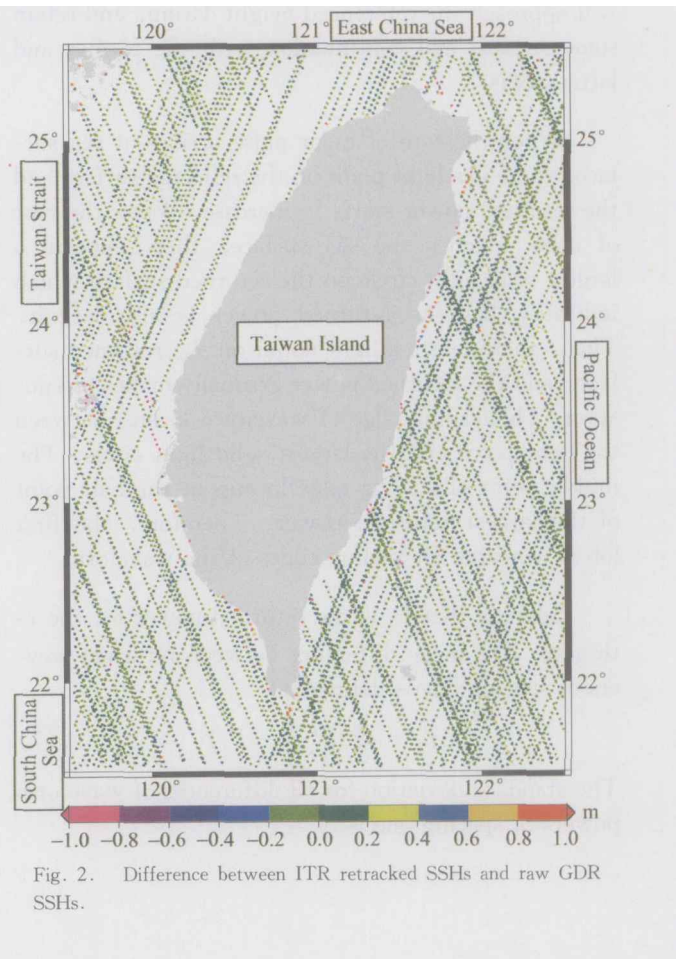


Fig. 2. Difference between ITR retracked SSHs and raw GDR SSHs.

Geosat is an American altimetry satellite, whose geodetic mission (GM) executed between Mar. 31, 1985 and Sep. 30, 1986, totally 549 days. National Oceanic and Atmospheric Administration (NOAA) provides GDRs and waveform data records (WDRs). GDRs provide 1 Hz altimetry data and environmental correction. WDRs include 10 Hz waveform data^[11]. Fig. 2 shows the distribution of Geosat/Gm track in the coastal water around Taiwan.

Waveforms of Geosat/GM in the coastal water around Taiwan are retracked with the β -5-parameter function fitting method, the threshold method and ITR, respectively, to verify the validity of ITR. The referenced geopotential model is GGM02C (2 to 200 degrees and orders)^[12] and EGM96 (201 to 360 degrees and orders)^[13]. The ocean tide is CSR4.0^[14].

The following two criterions are used to judge the success rate of retracking, and the difference between the retracked SSH and a modeled geoid height of the waveform retrackers.

The retracker with high retracking success rate is thought applicable in the test area. Applying the retracked range correction and all environmental corrections to GDRs, the retracked SSH can be obtained. Compared with the modeled local geoid height, smooth and consistent retracked SSH with the local geoid indicates good retracker. Table 1 shows the statistics of retracked results. The retracking success rate is the ratio of successfully retracked points and all altimetric points. As shown in Table 1, the success rate of linear β -5-parameter function fitting method is the lowest among the three retrackers, being only about 75%. The success rate of the threshold method is approximately the same as that of ITR. Compared with Taiwan's geoid^[15], the ITR retracked SSH has the highest accuracy, whose standard deviation is 0.235 m. The improved accuracy of ITR doubles those of β -5-parameter function-fitting method and threshold method, and is 3 times higher than the results of GDRs. Fig. 2 shows the difference between ITR retracked SSHs and raw GDR SSHs. There are some blanks without WDRs, especially in the west of Taiwan. Almost all of the differences are less than 0.2 meters. Bigger differences centralize mainly on the coastal water around Taiwan and other little islands. This indicates that the waveform in coastal water is seriously corrupted.

Table 1. Statistics of waveform retracking for GEOSAT/GM with different retrackers

Retracker	Retracking success rate (%)	Standard deviation (m)
GDRs	---	0.744
β -5-parameter	74.7	0.437
Threshold method	100.0	0.459
ITR	99.6	0.235

5 Conclusions

The waveform of satellite altimeter over coastal sea is corrupted by the topography and environment, which seriously decrease the accuracy of altimetry data. A new waveform retracking method ITR is put forward in this paper. WDRs and GDRs of Geosat/GM around Taiwan are processed with several retracking methods. The results indicate that ITR is obviously better than the β -5-parameter function fitting method and the threshold method. Therefore, ITR is more suitable for waveform retracking over coastal seas. ITR is useful for the study on geodesy, oceanography, geophysics and so on. The retracked altimetry data can be used to improve the tide model, the local gravity field model, the ocean current, and the wind field in the coastal region.

Acknowledgements The authors would like to thank J. Lillibridge for providing the Geosat/GM waveform data.

References

- 1 Bosch W. Geodetic application of satellite altimetry. In: Satellite Altimetry for Geodesy, Geophysics and Oceanography. Berlin, IAG Symposia, Springer-Verlag, 2004, 126: 3—21.
- 2 Fu L.L. and Cazenave A. Satellite Altimetry and Earth Sciences. San Diego, California: Academic Press, 2001.
- 3 Deng X.L. Improvement of geodetic parameter estimation in coastal regions from satellite radar altimetry. Thesis for Ph. D. Department of Spatial Sciences, Curtin University of Technology, 2004.
- 4 Brown G.S. The average impulse response of a rough surface and its application. IEEE Transactions on Antenna and Propagation, 1977, AP-25(1): 67—74.
- 5 Martin T.V., Zwally H.J., Brenner A.C. et al. Analysis and tracking of continental ice sheet radar altimeter waveforms. Journal of Geophysical Research, 1983, 88(C3): 1608—1616.
- 6 Wingham D.J., Rapley C.G. and Griffiths H. New techniques in satellite altimeter tracking systems. In: Proceedings of IGARSS'86 Symposium, Zurich, Sept., 1986, 1339—1344.
- 7 Bamber J.L. Ice sheet altimeter processing scheme. International Journal of Remote Sensing, 1994, 20: 48—54.
- 8 Davis C.H. A surface and volume scattering retracking algorithm for ice sheet satellite altimetry. IEEE Transactions on Geoscience and Remote Sensing, 1993, 31(4): 811—818.
- 9 Moritz H. Advanced Physical Geodesy. New York: Abacus Press, 1980.

- 10 Bettadpur S. V. and Eanes R. J. Geographical representation of radial orbit perturbations due to ocean tides; implications for satellite altimetry. *Journal of Geophysical Research*, 1994, 99; 24883—24894.
- 11 Lillibridge J. L., Smith W. H. F., Scharroo R. et al. The Geosat geodetic mission twentieth anniversary edition data product. In: AGU 2004 Fall Meeting, San Francisco, 2004.
- 12 GRACE home page. <http://www.csr.utexas.edu/grace/>. [2005.6.8]
- 13 Lemoine F. G., Kenyon S. C., Factor J. K. et al. The development of joint NASA GSFC and the National Imagery and Mapping Agency (NIMA) geopotential model EGM96. Report NASA/TP-1998-206861, National Aeronautics and Space Administration, Greenbelt, MD, 1998.
- 14 Eanes R. and Shuler A. Applications of an improved global tide model. Report T/P & Jason-1 SWT, NASA, Greenbelt, MD, 1999.
- 15 Hwang C. W., Guo J. Y., Liu Y. T. et al. Gravity anomalies in coastal waters from retracked Geosat/GM altimetry; comparison with shipborne and airborne gravity data. *Dynamic Planet 2005*, Australia, Aug. . 2005.